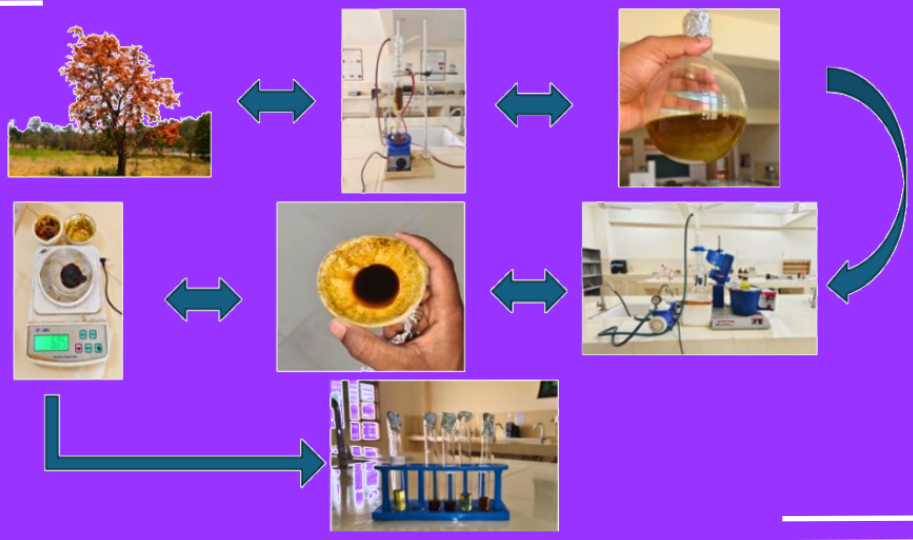

BJP

Bangladesh Journal of Pharmacology

Research Article

Effect of hydroethanolic extract of *Butea monosperma* flower on bleomycin-induced pulmonary fibrosis in mice via IL-6 modulation

A Journal of the Bangladesh Pharmacological Society (BDPS)
Journal homepage: www.bdpsjournal.org; www.banglajol.info
Abstracted/indexed in Academic Search Complete, Agroforestry Abstracts, Asia Journals Online, Bangladesh Journals Online, Biological Abstracts, BIOSIS Previews, CAB Abstracts, Current Abstracts, Directory of Open Access Journals, EMBASE/Excerpta Medica, Global Health, Google Scholar, HINARI (WHO), International Pharmaceutical Abstracts, Open J-gate, Science Citation Index Expanded, SCOPUS and Social Sciences Citation Index
Bangladesh J Pharmacol 2026; 21: 101-107
ISSN: 1991-0088

Effect of hydroethanolic extract of *Butea monosperma* flower on bleomycin-induced pulmonary fibrosis in mice via IL-6 modulation

Digvijay Singh[1], Shradha Bisht[1], and Mamta F. Singh[2]

[1]Department of Pharmacology, Uttaranchal Institute of Pharmaceutical Sciences, Uttaranchal University. Dehradun, Uttarakhand 248007, India; [2]Department of Pharmacology, College of Pharmacy, College of Engineering Roorkee, University, Roorkee, Uttarakhand 247667, India.

Article Info

Received: 8 July 2026
Accepted: 30 August 2026
Available Online: 11 September 2026

DOI: 10.3329/bjp.v21i3.91727

Cite this article:
Singh D, Bisht S, Singh MF. Effect of hydroethanolic extract of *Butea monosperma* flower on bleomycin-induced pulmonary fibrosis in mice via IL-6 modulation. Bangladesh J Pharmacol. 2026; 21: 101-107.

Abstract

This study evaluates the antifibrotic and anti-inflammatory potential of a hydroethanolic extract of *Butea monosperma* flowers in bleomycin-induced pulmonary fibrosis in Swiss albino mice. The extract (100 and 200 mg/kg orally) was administered for 21 days following oropharyngeal aspiration of bleomycin (2.5 mg/kg) and compared to pirfenidone (100 mg/kg). Parameters assessed included lung index, serum IL-6 levels, and histopathological architecture (Ashcroft scoring). Preliminary phytochemical screening confirmed the presence of flavonoids, phenolic compounds, tannins, and glycosides. The disease control group exhibited severe fibrosis (Ashcroft score: 5), elevated lung index (1.3 ± 0.0%), and increased IL-6 levels (6.1 ± 0.2 pg/mL). The extract at 200 mg/kg significantly ($p<0.001$) reduced the lung index to 1.0 ± 0.0% and IL-6 levels to 4.6 ± 0.2 pg/mL, with preserved pulmonary architecture (Ashcroft score: 1–2), demonstrating dose-dependent antifibrotic and anti-inflammatory effects superior to pirfenidone.

Introduction

Pulmonary fibrosis is a chronic, progressive, and often fatal form of interstitial lung disease characterized by disrupted matrix deposition and irreversible destruction of alveolar architecture (Barratt et al., 2018; Wang et al., 2024). Repeated injury to the alveolar epithelium, oxidative stress, and unchecked fibroblast activation and expansion of fibroblasts into myofibroblasts contribute to its pathogenesis (Leonard-Duke et al., 2020; Parimon et al., 2020).

Among the cytokines involved in chronic inflammation and fibrogenesis, interleukin-6 (IL-6) is a pleiotropic cytokine that primarily acts on vascular cells, while Transforming Growth Factor-beta (TGF-β1) plays a central role in fibrogenesis (Ding et al., 2022; Shieh et al., 2019). IL-6 expression is increased in multiple animal models of pulmonary fibrosis, including bleomycin-induced damage, and fibrosis is driven mainly by activation of its downstream STAT3 signaling pathway rather than the ERK pathway (Chen et al., 2023).

Standard-of-care drug therapy for the clinical management of pulmonary fibrosis currently consists of FDA-approved antifibrotic drugs, pirfenidone and nintedanib (Glass et al., 2022; Yang et al., 2024). While these agents can significantly slow the decline in pulmonary function, they do not treat or reverse the disease process (Savin et al., 2022). Furthermore, their clinical use is largely limited by various adverse effects, such as gastrointestinal intolerance, hepatotoxicity, and photo-

toxicity. This therapeutic plateau highlights the urgent clinical need for alternative, multi-targeted therapies, particularly those derived from natural phytotherapeutic sources, which may offer holistic efficacy with improved safety profiles (Wang et al., 2024).

Natural products are well known for their pharmacological effects, and many medicinal plants have demonstrated strong therapeutic benefits against pulmonary fibrosis in experimental animals. For example, the active sesquiterpene component bilobalide from *Ginkgo biloba* has shown significant protective effects against bleomycin-induced pulmonary inflammation and extracellular matrix deposition in vivo (Zhang et al., 2023). *Marrubium vulgare*, a polyphenol-rich wild herb, has been reported to provide in vivo protection against experimental pulmonary inflammation, oxidative stress, and subsequent fibrosis through an aqueous extract enriched with high levels of catechin, chlorogenic acid, and caffeic acid (Abidi et al., 2022). This finding aligns with recent observations where active pentacyclic triterpenes, including asiatic acid and asiaticoside from *Centella asiatica*, exhibited potent antifibrotic efficacy by mitigating Smad3-mediated matrix expression and structural lung damage in a similar rat model system (Soeroso et al., 2024).

Butea superba has been the subject of several pharmacological investigations, particularly concerning the male reproductive and vascular systems. In experimental models, its active extracts significantly increase the frequency of penile erections and intracavernous pressure in both normal and diabetic in vivo models. The primary mechanism of action for this erectile enhancer is likely the relaxation of cavernosal smooth muscle, mediated through the inhibition of cAMP and cGMP phosphodiesterase pathways (Tocharus et al., 2006, 2012). In addition to its vasodilatory effects, *B. superba* also exhibits dose-dependent androgenic activities. Optimal therapeutic doses have been shown to increase testis weight and sperm count (Manosroi et al., 2006). However, chronic exposure to extremely high doses has been associated with disruption of testosterone levels and liver enzyme function (Cherdshewasart et al., 2008).

B. monosperma (Lam.) Taub. (Flame of the Forest) is a well-known and valuable medicinal plant widely used in folk medicine, recognized for its potent anti-inflammatory, antioxidant, and tissue-protective properties (Jain and Dubey, 2023; Kumari et al., 2022). This plant is particularly rich in bioactive secondary metabolites, including flavonoids (butrin and isobutrin), tannins, and glycosides (Sudhakar Rao et al., 2024). Previous pharmacological studies have shown that *B. monosperma* exerts its anti-inflammatory effects by downregulating TNF-α and IL-6 (Rasheed et al., 2010; Zahra et al., 2024), indicating significant potential for ameliorating the complex, multifaceted pathogenesis of pulmonary fibrosis. Notably, butein, the major flavonoid of *B. monosperma*, has been demonstrated to individually inhibit TGF-β, NF-κB, and downstream MAPK (p38/JNK) signaling pathways, as well as reduce oxidative stress in hepatic stellate cell models of fibrosis (Szuster-Ciesielska et al., 2013). It also exhibits high free-radical-scavenging activity when isolated directly from *B. monosperma* flower extract (Sehrawat and Kumar, 2012). The leaf extracts of *B. monosperma* have shown potent antioxidant and antidiabetic effects by inhibiting α-amylase and α-glucosidase enzymes, activities attributed to apigenin derivatives and vanillic acid (Farooq et al., 2020). Additionally, palasonin, a bioactive compound isolated from *B. monosperma* seeds, has demonstrated substantial anthelmintic activity against *Haemonchus contortus* by inhibiting glutamate dehydrogenase and tubulin proteins (Rahal et al., 2022). The flavonoid isocoreopsin, isolated from *B. monosperma* flowers, has exhibited potent chemopreventive activity against colorectal and hepatocellular carcinoma cell lines by inhibiting the formation of aberrant crypt foci (Subramaniyan et al., 2016). Furthermore, network pharmacology studies have revealed that *B. monosperma* stem bark modulates critical inflammatory targets such as NF-κB, AKT1, and MAPK1, supporting its traditional use in treating inflammatory bowel conditions (Mondal et al., 2025). Specifically, the aqueous extract of *B. monosperma* flowers demonstrated considerable dose-dependent hepatoprotection against CCl_4-induced liver injury by restoring aberrant biochemical and histological markers toward normalcy (Sharma and Shukla, 2011). The intratracheal bleomycin model in mice is widely regarded as the most well-characterized animal model for preclinical testing of treatments for pulmonary fibrosis (Jenkins et al., 2017).

Hence, the present investigation utilized the hydroethanolic extract of *B. monosperma* flower to evaluate its antifibrotic and anti-inflammatory potential in a bleomycin-induced pulmonary fibrosis murine model. The extract's effects were directly compared to pirfenidone, which served as the standard clinical drug for positive control.

Materials and Methods

Study subjects

Seventy-two patients with NSCLC who underwent surgical treatment at the Qingpu Branch of Zhongshan Hospital, Fudan University, between December 2018 and December 2020 were enrolled. Tumor tissues and matched adjacent non-tumor tissues (located ≥ 3 cm from the lesion) were collected during surgery and immediately preserved. All specimens were pathologically verified. Inclusion criteria: NSCLC confirmed by histopathology; no history of other malignancies; and no prior anti-cancer treatment before enrollment. Exclusion criteria: Presence of any additional malignant tumors; refusal to provide tissue samples for research;

and lung lesions originating from non-primary metastatic tumors.

Cell culture

The NSCLC cell lines A549, H1299, and H460, along with the bronchial epithelial cell line BEAS-2B, were obtained from the American Type Culture Collection (ATCC, USA). Cells were cultured in DMEM (Thermo Fisher Scientific, USA) supplemented with 10% fetal bovine serum (Gibco, USA) and standard concentrations of penicillin (100 U/mL) and streptomycin (100 μg/mL). Cultures were maintained under routine conditions—namely, a humidified atmosphere with 5% CO_2 at 37°C. Passaging was performed when the cell monolayer reached approximately 80% confluence (Zhang et al., 2022).

Cell transfection and experimental grouping

Synthetic miR-370-5p mimic, inhibitor, and their respective negative controls (NCs) were obtained from RiboBio (Guangzhou, China). The KPNA3 overexpression construct (pcDNA3.1-KPNA3, abbreviated as pc-KPNA3) and the empty pcDNA3.1 vector were purchased from GenePharma (Shanghai, China). Once the cells reached approximately 80% adherence, they were detached using trypsin and prepared for transfection. Lipofectamine 2000 (Invitrogen, USA) was used according to the manufacturer's instructions. Subsequent assays were performed 48 hours post-transfection (Zhang et al., 2019).

Cells were allocated into the following groups: Blank, mimic NC, miR-370-5p mimic, inhibitor NC, miR-370-5p inhibitor, miR-370-5p mimic + pcDNA3.1, and miR-370-5p mimic + pc-KPNA3.

RT-qPCR

Total RNA from cultured cells and tissue samples was isolated using TRIzol reagent (Invitrogen, USA). RNA quantity and purity were assessed immediately after extraction. Reverse transcription was performed using the PrimeScript™ RT reagent kit (Takara, China), and the resulting cDNA was stored at −20°C until analysis. Primer sequences for miR-370-5p and KPNA3 were designed and synthesized by Genechem (China). Quantitative PCR was conducted on an ABI 7500 real-time PCR system (ABI, USA) using Power SYBR™ Green PCR Master Mix (Thermo Fisher Scienti-fic). U6 served as the internal reference for miR-370-5p, while GAPDH was used for KPNA3 normalization. Relative gene expression levels were calculated using the 2-ΔΔCt method (Sun et al., 2022).

Western blot analysis

Proteins from cultured cells were harvested using RIPA buffer (Beyotime). Protein concentration was quantified with a BCA assay (Beyotime) according to the manufacturer's protocol. Equal amounts of lysates (30 μg per sample) were resolved on 10% SDS–polyacrylamide gels and transferred onto PVDF membranes (Sigma, USA) using a semi-dry transfer system. Membranes were blocked at room temperature with 5% skim milk (Beyotime) before overnight incubation at 4°C with primary antibodies: KPNA3 (1:1000, Bethyl Laboratories, USA) and GAPDH (1:5000, Proteintech). After three washes with TBST, membranes were incubated with HRP-conjugated goat anti-rabbit secondary antibody (1:1000, Abcam) for 1 hour at room temperature. Following additional washes, bands were visualized using an enhanced chemiluminescent reagent (Beyotime). GAPDH served as the loading control, and densitometric measurements were obtained using ImageJ (Zhao et al., 2021).

CCK-8 assay

Cells in the exponential growth phase were rinsed with PBS and detached from culture flasks using a mild trypsin treatment. The resulting suspension was gently triturated to obtain a single-cell suspension, which was then counted and diluted to approximately 2×10^4 cells/mL. Approximately 2×10^3 cells were seeded into each well of a 96-well microplate. Cell viability was assessed using the CCK-8 reagent (Dojindo, Japan). At the indicated time intervals (0, 24, 48, and 72 hours), 10 μL of the reagent was added to each well, followed by a 1-hour incubation. Optical density at 450 nm was measured using a microplate reader to quantify metabolic activity (Xu et al., 2025).

Flow cytometry

Cells harvested during exponential growth were gently detached using EDTA-free trypsin (Bioss, China), collected into flow cytometry tubes, and pelleted by centrifugation. After discarding the supernatant, the cells were rinsed three times with chilled PBS and resuspended to obtain a uniform suspension. Apoptotic events were quantified using an annexin V-FITC/PI dual-staining kit (Beyotime). For staining, 5 μL of Annexin V-FITC and 10 μL of PI were added to the cell suspension and incubated for 15 min at room temperature in the dark. Samples were subsequently analyzed on a flow cytometer (BD Biosciences, USA) (Shen et al., 2021).

Transwell assay

Cell motility was evaluated using a Transwell migration system (Becton Dickinson, USA). Post-transfection cells in the logarithmic growth phase were harvested, washed twice with serum-free medium, resuspended, and counted. A total of 5×10^4 cells were seeded into the upper chamber containing serum-free medium, while the lower chamber was filled with 500 μL of RPMI-1640 supplemented with 20% FBS as a chemoattractant. The inserts were incubated at 37°C for 24 hours. After incubation, non-migrated cells on the upper membrane surface were gently removed. The

chambers were rinsed with PBS, and migrated cells on the underside of the membrane were fixed with 4% paraformaldehyde for 10 min and stained with crystal violet. Images were captured using a light microscope, and migrated cells were quantified using ImageJ (Liao and Peng, 2020).

Dual luciferase reporter gene assay

The potential interaction between miR-370-5p and the 3′ UTR of KPNA3 was initially predicted using the target-Scan database (https://www.targetscan.org/vert_72/). Based on the predicted binding motif, DNA fragments containing the wild-type KPNA3 3′UTR sequence were synthesized and inserted downstream of a luciferase reporter to generate the KPNA3-WT construct. A corresponding mutant reporter (KPNA3-MUT), in which the predicted miRNA binding site was specifically altered, was generated in parallel. A549 cells in logarithmic growth phase were seeded into 96-well plates, and when the monolayers reached approximately 70% confluence, reporter constructs (WT or MUT) were co-transfected with either the miR-370-5p mimic or the matched NC using Lipofectamine 2000. After 48 hours of incubation, cells were lysed and subjected to a dual-luciferase assay. Firefly luciferase activity was normalized to Renilla activity (Wang et al., 2024).

Statistical analysis

All analyses were performed using SPSS 25.0 (IBM, USA) and Graphad Prism 9.5 (GraphPad Software, USA). Numerical data were assessed for normality and homogeneity of variance prior to statistical testing. Data are presented as mean ± SD. Comparisons between two groups were conducted using independent-sample t-tests, while comparisons among multiple groups were evaluated using one-way ANOVA, followed by Tukey's post-hoc test for pairwise comparisons when appropriate.

Results

Percentage yield

The yield of semi-solid mass of *B. monosperma* extract was 20.2% w/w.

Phytochemical screening

The results of preliminary phytochemical screening of extract of *B. monosperma* flower showed the presence of flavonoids, phenolic compounds, tannins and glycosides. The extract contained multiple classes of polyphenolic compounds.

Effects on lung index

The lung index of the disease control group was significantly higher (1.3 ± 0.0%, $p<0.001$) than that of the normal control group (0.5 ± 0.0%). Administration of the extract attenuated this pathological increase in a dose-dependent manner. In the 100 mg/kg extract group, the lung index was significantly reduced to 0.8 ± 0.0% ($p<0.001$), whereas the 200 mg/kg reduced the ratio down to 1.0 ± 0.0%. Interestingly, the 100 mg/kg dose resulted in a greater reduction of the lung index compared to the 200 mg/kg dose, suggesting that the extract may preferentially attenuate pulmonary edema at lower doses (Table I).

Modulation of interleukin-6 (IL-6) levels

Bleomycin administration led to a significant increase in IL-6 levels (6.1 ± 0.2 pg/mL, $p<0.01$) compared with healthy controls (5.3 ± 0.2 pg/mL). Oral administration of the extract effectively attenuated this inflammatory response. IL-6 levels significantly decreased to 4.6 ± 0.2 pg/mL ($p<0.001$) following treatment with a 200 mg/kg dose of the extract, demonstrating a greater anti-inflammatory effect than pirfenidone (5.1 ± 0.2 pg/mL) (Table I).

Histopathological study and Ashcroft scoring

Normal control Hematoxylin and Eosin staining of lung sections from the normal control group showed intact alveoli with thin septa (Ashcroft score: 0) (Table I). In contrast, lungs in the disease control group demonstrated extensive abnormalities in lung architecture, including heavy inflammatory cell infiltration and significant thickening of alveolar septa, as indicated by an Ashcroft score of 5. Pirfenidone treatment markedly restored the pulmo-nary architecture, as reflected by a decreased Ashcroft score of 1–2.

The extract treatment provided significant protection against bleomycin-induced injury. At a dose of 100 mg/

Table I

Effect of *B. monosperma* on different parameters in bleomycin-induced pulmonary fibrosis

Treatment	Lung index (%)	IL-6 (pg/mL)	Ashcroft score
Normal control	0.5 ± 0.0	5.3 ± 0.2	0
Disease control (bleomycin, 2.5 mg/kg)	1.3 ± 0.0[b]	6.1 ± 0.2	5
Pirfenidone (100 mg/kg)	0.6 ± 0.0[b]	5.1 ± 0.2[b]	1-2[a]
Extract (100 mg/kg)	0.8 ± 0.0[b]	5.2 ± 0.2[b]	2-3[b]
Extract (200 mg/kg)	1.0 ± 0.0[b]	4.6 ± 0.2[b]	1-2[b]

The statistical significance of difference between means was calculated by ANOVA. Values are expressed in terms of mean ± SEM

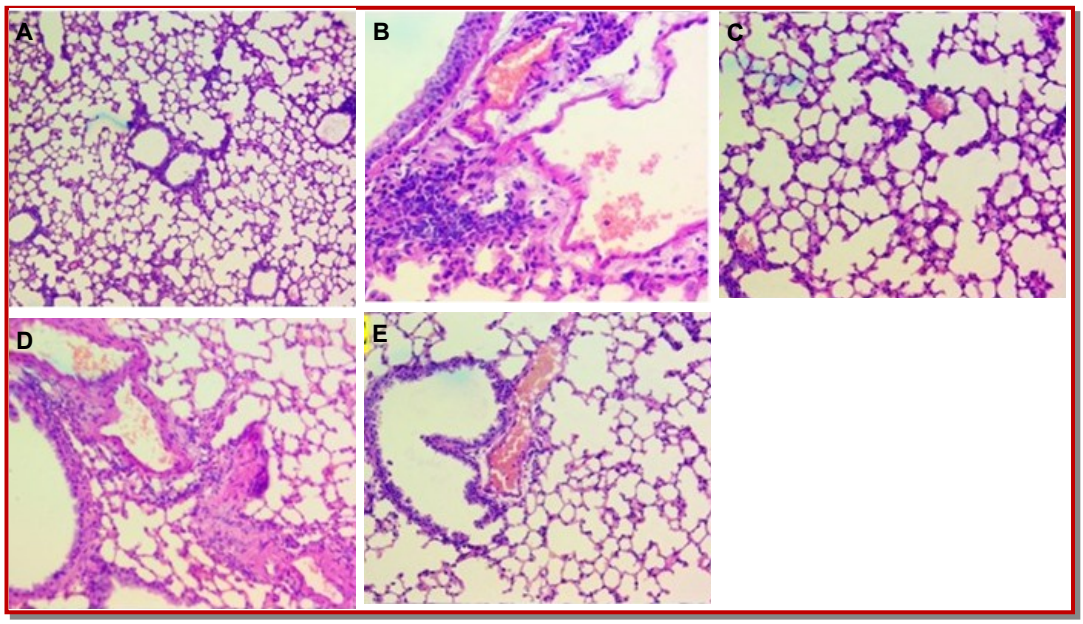

Figure 1: Histopathological evaluation of lung tissues. Normal control (A), Disease control (B), Standard treatment, pirfenidone (C), extract 100 mg/kg (D), and extract 200 mg/kg (E)

kg, the extract partially preserved alveolar structures and significantly reduced septal thickening compared to the disease control group (Ashcroft score: 2–3). Notably, the 200 mg/kg dose of the extract demonstrated substantial tissue protection, characterized by open alveolar spaces, minimal inflammatory infiltration, and limited fibrotic remodeling, comparable to standard therapy, resulting in an Ashcroft score of 1–2 (Figure 1).

Discussion

The current research demonstrates that the phytochemical profile of the hydroethanolic extract of *B. monosperma* flowers is consistent with previously reported studies on *B. monosperma* flowers. This finding provides a mechanistic rationale for its antioxidant and anti-inflammatory activities, possibly due to synergistic interactions among the phenolic compounds within the extract. The extract exhibits considerable antifibrotic and anti-inflammatory properties in mice with bleomycin-induced lung fibrosis. Bleomycin injection produced significant pathological alterations in the disease control group, including an increased lung index (1.3 ± 0.0%), elevated serum IL-6 levels (6.1 ± 0.2 pg/mL), and severe architectural distortion (Ashcroft score: 5). Administration of the extract mitigated these alterations in a dose-dependent fashion: the dose of 200 mg/kg decreased the lung index to 1.0 ± 0.0% and IL-6 to 4.6 ± 0.2 pg/mL, while preserving pulmonary struc-ture (Ashcroft score: 1–2), comparable to the reference medication pirfenidone. Notably, the 200 mg/kg dose resulted in a more substantial decrease in IL-6 compared to pirfenidone (4.6 vs. 5.1 pg/mL), although the 100 mg/kg dose exhibited a relatively greater reduction in lung index than the higher dose, indicating that the two dosages may exert varying efficacy across different parameters. The lung index is a quantitative marker of pulmonary edema and fibrotic tissue deposition. These findings generally align with and extend earlier reports on *B. monosperma* and its related phytoconstituents. The significant IL-6 reduction observed here supports this mechanism, as Rasheed et al. (2010) demonstrated that butrin, isobutrin, and butein—major flavonoids of *B. monosperma*—selectively inhibit NF-κB activation in mast cells, thereby lowering TNF-α, IL-6, and IL-8 levels. Similarly, butein suppresses TGF-β, NF-κB, and MAPK (p38/JNK) signaling in hepatic stellate cells, suggesting a possible antifibrotic effect of the same compound in the lung (Szuster-Ciesielska et al., 2013). The histological protection observed with BME is consistent with findings from other phytotherapeutics in this model, such as bilobalide from *Ginkgo biloba* (Zhang et al., 2023), supporting the broader hypothesis that flavonoid-rich natural extracts can modulate bleomycin-induced fibrotic remodeling. However, unlike pirfenidone and nintedanib, which primarily act through specific pathways such as JAK2 inhibition (Yang et al., 2024) and are limited by significant gastrointestinal and hepatic toxicity (Savin et al., 2022), the extract appears to achieve similar or superior efficacy through multi-target phytochemical actions without the adverse effect profile associated with these standard agents. Reason: Corrected grammar, punctuation, and spelling errors; improved sentence structure and clarity; enhanced vocabulary for technical accuracy and readability; and ensured consistent use of scientific terminology without altering the original meaning.

The potential mechanism underlying these effects can be attributed to the polyphenolic composition of the extract, which includes flavonoids (butrin, isobutrin), tannins, and glycosides. IL-6 has been reported to mediate fibroblast activation primarily through the STAT3 signaling pathway in bleomycin-induced fibrosis (Chen et al., 2023). The significant inhibition of IL-6 by BME suggests interference with this inflammatory cascade, possibly via inhibition of NF-κB, consistent with the proposed mechanisms of butrin and isobutrin (Rasheed et al., 2010). Additionally, the antioxidant activity of these phenolic compounds (Sehrawat and Kumar, 2012) may neutralize reactive oxygen species generated during bleomycin-induced alveolar damage, thereby preventing the oxidative trigger for fibroblast-to-myofibroblast transition.

The limitations of this study include: a) the findings may not be directly extrapolated to other fibrosis models, species, or chronic/repetitive injury settings; b) the proposed mechanisms—polyphenolic, multi-target, antioxidant, and anti-inflammatory—remain inferential and have not been confirmed by pathway-specific assays; c) the extract was not standardized to specific marker compounds nor quantified using chromatographic methods; and (d) the exact upstream molecular targets (e.g., TGF-β1/Smad signaling) were not directly investigated.

Conclusion

The hydroethanolic extract of *B. monosperma* flower has antifibrotic and anti-inflammatory agent, effectively reducing IL-6 expression and protecting pulmonary architecture with effects comparable or superior to pirfenidone.

Financial Support

Institutional

Ethical Issue

The Institutional Animal Ethics Committee (Approval no IAEC/UIPS/MPL/03/2025) approved the experimental protocol that was carried out under CCSEA guidelines

Conflict of Interest

Authors declare no conflict of interest

Acknowledgements

The authors would like to thank Mr. Jitender Joshi, Chancellor, and Prof. Dharam Buddhi, Vice Chancellor of Uttaranchal University, Dehradun, for encouraging the publication of this work. Authors also like to thank Director UIPS Prof. Vikas Jakhmola for his valuable suggestions

References

Abidi A, Dhaouafi J, Brinsi C, Tounsi H, Sebai H. Tunisian horehound (*Marrubium vulgare*) aqueous extract improves treatment of bleomycin-induced lung fibrosis in rat. Dose Response. 2022; 20: 15593258221119300.

Barratt S, Creamer A, Hayton C, Chaudhuri N. Idiopathic pulmonary fibrosis (IPF): An overview. J Clin Med. 2018; 7: 201.

Chen Y, Zhou J, Xu S, Nie J. Role of interleukin-6 family cytokines in organ fibrosis. Kidney Dis. 2023; 9: 239-53.

Cherdshewasart W, Bhuntaku P, Panriansaen R, Dahlan W, Malaivijitnond S. Androgen disruption and toxicity tests of *Butea superba* Roxb., a traditional herb used for treatment of erectile dysfunction, in male rats. Maturitas 2008; 60: 131-37.

Ding Y, Hou Y, Liu Y, Yu T, Cui Y, Nie H. MiR-130a-3p alleviates inflammatory and fibrotic phases of pulmonary fibrosis through proinflammatory factor TNF-α and profibrogenic receptor TGF-βRII. Front Pharmacol. 2022; 13: 863646.

Farooq MU, Mumtaz MW, Mukhtar H, Rashid U, Akhtar MT, Raza SA, Nadeem M. UHPLC-QTOF-MS/MS based phytochemical characterization and anti-hyperglycemic prospective of hydro-ethanolic leaf extract of *Butea monosperma*. Sci Rep. 2020; 10: 3530.

Glass DS, Grossfeld D, Renna HA, Agarwala P, Spiegler P, DeLeon J, Reiss AB. Idiopathic pulmonary fibrosis: Current and future treatment. Clin Respir J. 2022; 16: 84-96.

Heinemann F, Birk G, Schoenberger T, Stierstorfer B. Deep neural network based histological scoring of lung fibrosis and inflammation in the mouse model system. PLoS ONE. 2018; 13: e0202708.

Hosseini S, Imenshahidi M, Hosseinzadeh H, Karimi G. Effects of plant extracts and bioactive compounds on attenuation of bleomycin-induced pulmonary fibrosis. Biomed Pharmacother. 2018; 107: 1454-65.

Jain S, Dubey PK. *Butea monosperma* (Lam.) Taub: Review on its chemistry, morphology, ethnomedical uses, phytochemistry and pharmacological activities. J Drug Deliv Ther. 2023; 13: 137-44.

Jenkins RG, Moore BB, Chambers RC, Eickelberg O, Konigshoff M, Kolb M, Laurent GJ, Nanthakumar CB, Olman MA, Pardo A, Selman M, Sheppard D, Sime PJ, Tager AM, Tatler AL, Thannickal VJ, White ES. An official American Thoracic Society workshop report: Use of animal models for the preclinical assessment of potential therapies for pulmonary fibrosis. Am J Respir Cell Mol Biol. 2017; 56: 667-79.

Kumari P, Raina K, Thakur S, Sharma R, Cruz-Martins N, Kumar P, Barman K, Sharma S, Kumar D, Prajapati PK, Sharma R. Ethnobotany, phytochemistry and pharmacology of palash (*Butea monosperma* (Lam.) Taub.): A systematic review. Curr Pharmacol Rep. 2022; 8: 188-204.

Leonard-Duke J, Evans S, Hannan RT, Barker TH, Bates JHT, Bonham CA, Moore BB, Kirschner DE, Peirce SM. Multiscale models of lung fibrosis. Matrix Biol. 2020; 91-92: 35-50.

Maheshwaran L, Nadarajah L, Senadeera SPNN, Ranaweera CB, Chandana AK, Pathirana RN. Phytochemical testing methodologies and principles for preliminary screening/ qualitative testing. Asian Plant Res J. 2024; 12: 11-38.

Manosroi A, Sanphet K, Saowakon S, Aritajat S, Manosroi J. Effects of *Butea superba* on reproductive systems of rats. Fitoterapia 2006; 77: 435-38.

Mondal S, Ganguly A, Nandi A, Das A, Mondal S, Mukherjee S, Pawar SD, Dey YN. Network pharmacology and molecular docking reveal multi-target mechanisms of *Butea monosperma* stem bark extract in ulcerative colitis. Sci Rep. 2025; 15: 40302.

Parimon T, Yao C, Stripp BR, Noble PW, Chen P. Alveolar epithelial type II cells as drivers of lung fibrosis in idiopathic pulmonary fibrosis. Int J Mol Sci. 2020; 21: 2269.

Rahal A, Sharma DK, Kumar A, Sharma N, Dayal D. *In silico* to *in vivo* development of a polyherbal against *Haemonchus contortus*. Heliyon. 2022; 8: e08789.

Rasheed Z, Akhtar N, Khan A, Khan KA, Haqqi TM. Butrin, isobutrin, and butein from medicinal plant *Butea monosperma* selectively inhibit nuclear factor-κB in activated human mast cells: Suppression of tumor necrosis factor-α, interleukin (IL) -6, and IL-8. J Pharmacol Exp Ther. 2010; 333: 354-63.

Savin IA, Zenkova MA, Senkova AV. Pulmonary fibrosis as a result of acute lung inflammation: Molecular mechanisms, relevant *in vivo* models, prognostic and therapeutic approaches. Int J Mol Sci. 2022; 23: 14959.

Sehrawat A, Kumar V. Butein imparts free radical scavenging, anti-oxidative and proapoptotic properties in the flower extracts of *Butea monosperma*. Biocell 2012; 36: 63-71.

Sharma N, Shukla S. Hepatoprotective potential of aqueous extract of *Butea monosperma* against CCl_4 induced damage in rats. Exp Toxicol Pathol. 2011; 63: 671-76.

Shieh J-M, Tseng H-Y, Jung F, Yang S-H, Lin J-C. Elevation of IL-6 and IL-33 levels in serum associated with lung fibrosis and skeletal muscle wasting in a bleomycin-induced lung injury mouse model. Mediators Inflamm. 2019; 2019: 1-12.

Soeroso N, Ichwan M, Wahyuni A, Mariedina C, Pakpahan Y. Bleomycin-induced fibrosis and the effectiveness of *Centella asiatica* as a treatment. J Exp Pharmacol. 2024; 16: 311-20.

Subramaniyan B, Polachi N, Mathan G. Isocoreopsin: An active constituent of n-butanol extract of *Butea monosperma* flowers against colorectal cancer (CRC). J Pharm Anal. 2016; 6: 318-25.

Sudhakar Rao SVD, Ryntathiang I, Behera A, Saravanan S, Prasad M, Dharmalingam Jothinathan MK. Comparative in vitro and in silico analyses of phytochemicals from *Butea monosperma* for wound-healing potential in human cells. Cureus. 2024.

Szuster-Ciesielska A, Mizerska-Dudka M, Daniluk J, Kandefer-Szerszen M. Butein inhibits ethanol-induced activation of liver stellate cells through TGF-β, NFκB, p38, and JNK signaling pathways and inhibition of oxidative stress. J Gastroenterol. 2013; 48: 222-37.

Tocharus C, Smitasiri Y, Jeenapongsa R. *Butea superba* Roxb. enhances penile erection in rats. Phytother Res. 2006; 20: 484-89.

Tocharus C, Sooksaen P, Shimbhu D, Tocharus J. *Butea superba* (Roxb.) improves penile erection in diabetic rats: *B. superba* improves penile erection. Andrologia. 2012; 44: 728-33.

Wang J, Li K, Hao D, Li X, Zhu Y, Yu H, Chen H. Pulmonary fibrosis: Pathogenesis and therapeutic strategies. Med Comm. 2024; 5: e744.

Yang Y, Wang X, Zhang J. Pirfenidone and nintedanib attenuate pulmonary fibrosis in mice by inhibiting the expression of JAK2. J Thorac Dis. 2024; 16: 1128-40.

Zahra N, Mazhar A, Zahid B, Naeem MA, Sarwar A, Aziz T, Alharbi M, Albekairi TH, Alasmari AF. Evaluation of influence of *Butea monosperma* floral extract on inflammatory biomarkers. Open Chem. 2024; 22: 20230199.

Zhang L, Qu S, Wang L, Wang C, Yu Q, Zhang Z, Diao Y, Zhang B, Li Y, Shi Y, Wang P. Tianlongkechuanling inhibits pulmonary fibrosis through down-regulation of arginase-ornithine pathway. Front Pharmacol. 2021; 12: 661129.

Zhang X, Zhang W, Chen X, Cai Y. Prevention of bleomycin-induced pulmonary inflammation and fibrosis in mice by bilobalide. Evid Based Complement Alternat Med. 2023; 2023: 1973163.

Zhou X, Moore B. Lung section staining and microscopy. Bio-Protoc. 2017; 7.

Author Info

Shradha Bisht (Principal contact)
e-mail: itsshradha30@gmail.com